

## Shear driven solitary waves on a liquid film

A. M. Frank

*Institute of Computational Modeling SB RAS, Krasnoyarsk, 660036, Russia*

(Received 10 July 2006; revised manuscript received 16 October 2006; published 5 December 2006)

Long nonlinear two-dimensional traveling waves on a film driven by laminar gas flow are investigated numerically via solving Navier-Stokes equations. The evolution of their shape, amplitude, and speed with increasing Reynolds number is studied. The existence of solitary waves is demonstrated. A comparison between shear driven and gravity-capillary waves is made and discussed. It is shown that shear driven waves as compared to gravity driven waves are much higher for equal film Reynolds numbers and much slower for equal wave amplitudes.

DOI: 10.1103/PhysRevE.74.065301

PACS number(s): 47.15.gm, 47.35.De

Since the pioneering work of Kapitza and Kapitza [1], gravity-capillary waves have been extensively investigated both experimentally and numerically. Detailed experimental studies of forced regular waves, including solitary waves, have been made [2–4]. Numerous numerical simulations including direct numerical solution of Navier-Stokes equations [5–7] have been performed. On the contrary, nonlinear waves driven on the film surface by gas flow are much less investigated. Gas sheared liquid films are encountered in numerous technological processes and play an essential role in many devices for ground and space applications.

There are many works dealing with the problem of linear and weakly nonlinear stability for two-layer flow. A review of the latest results can be found elsewhere [8–10]. Many fewer papers consider strongly nonlinear shear driven waves. They have been studied mainly experimentally [11–15]. Only natural waves have been considered, which are often three dimensional and quite irregular. There are no experiments on forced regular waves like the experiments cited above on gravity waves. We are aware of numerical investigations [16,17], but they studied two-layer flows with parameters essentially different—i.e., not gas driven liquid films. Some nonlinear wave regimes in gas-film systems were also studied in Refs. [8,10,18], in particular in connection with a flooding problem. As for the solitary waves, only the authors of Refs. [13,14] considered some large amplitude waves as being solitary, though their photographs and surface tracings are not as convincing as those obtained for the gravity-capillary solitary waves [1–3]. Craik [12] observed some very long waves for the thin films (he called them “slow waves”), which one might assume to be solitary ones, but there is not enough evidence for that conclusion. Demekhin [18] reported that no solitary waves were obtained among nonlinear solutions for the gas-film system. The objective of this work is, therefore, to investigate if solitary waves can exist in gas driven liquid film and to compare their characteristics with that of well-studied gravity-capillary waves.

The statement of the problem is as follows. Two-dimensional (2D) thin-film flow is driven by gas flow in a channel (Fig. 1). The gas is assumed to be incompressible. We also consider gas flow with moderate Reynolds number, so it is assumed to be laminar. The density and kinematic viscosity of the liquid and gas are equal to  $\rho_1, \nu_1$  and  $\rho_2, \nu_2$ , respectively. We use the thickness  $h$  of undisturbed film as a length scale and also the viscous time scale  $h^2/\nu_1$ . Then, the

whole two-phase flow is governed by the following dimensionless equations:

$$\rho \frac{D\mathbf{u}}{Dt} = \text{div } P + \text{We } K \delta(\eta) \mathbf{n} + \rho G \mathbf{e}_g, \quad (1)$$

$$\text{div } \mathbf{u} = 0, \quad (2)$$

$$P = -pI + 2\rho\nu S. \quad (3)$$

Here  $D/Dt = \partial/\partial t + \mathbf{u} \cdot \nabla$  is the material derivative,  $P$  is the Navier-Stokes stress tensor,  $S$  is the strain rate tensor,  $\text{We} = \frac{\sigma_0 h}{\rho \nu_1^2}$  is the Weber number ( $\sigma_0$  is the surface tension),  $K$  is twice the mean curvature of the interface,  $\delta(\eta)$  is the delta function of  $\eta = (y - f(t, x)) / \sqrt{1 + f_x^2}$ ,  $y = f(t, x)$  is the equation of the interface,  $\mathbf{n}$  is the unit normal,  $G = gh^3/3\nu_1^2$  is the Galileo number ( $g$  is the gravity acceleration),  $\mathbf{e}_g$  is the unit vector directed along the gravity force, and  $\rho$  and  $\nu$  are the piecewise constant dimensionless density and kinematic viscosity, which are equal to unity for the liquid and to  $\rho_2/\rho_1$  and  $\nu_2/\nu_1$  for the gas, respectively.

A numerical method of particles for incompressible fluid is used [19] that is a conservative combination of the particle approach and Galerkin method. A detailed description of the method, including applications to film flows, can be found elsewhere [20,21]. Here we just briefly outline some peculiarities that are characteristics of the problem under consideration. We investigate periodic 2D waves; therefore, the flow is assumed to be periodic in the streamwise direction. No-slip boundary conditions hold at the channel walls. The stress continuity at the interface is naturally approximated

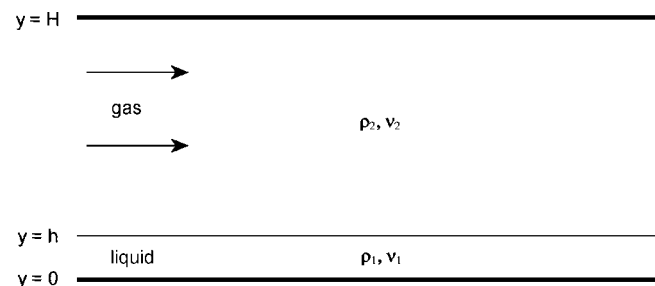


FIG. 1. Sketch of the flow.

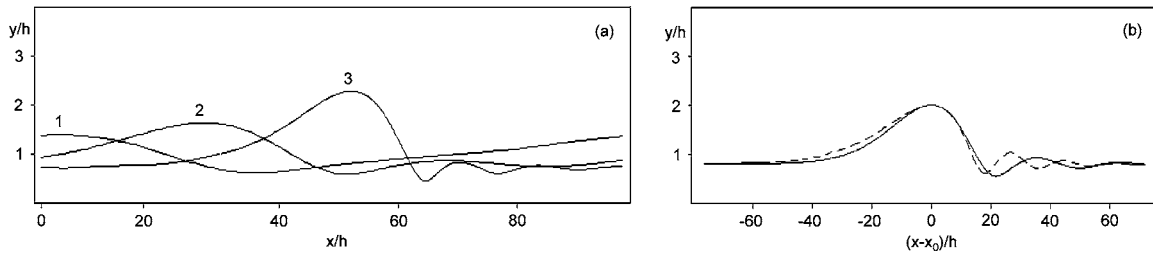


FIG. 2. Profiles of stationary shear driven waves: (a) dimensionless wavelength  $L=100$ , (1)  $Re_g=580$ ,  $Re_f=2.9$ , (2)  $Re_g=830$ ,  $Re_f=4.8$ , and (3)  $Re_g=1470$ ,  $Re_f=13.8$  and (b) wavelength  $L=200$ ; solid line, shear driven wave at  $Re_g=830$ ; dashed line, gravity wave at  $G=26$ ;  $x_0$ , abscissa of the wave crest.

due to the Galerkin method implementation. Nevertheless, in order to obtain a more accurate approximation and to avoid Gibbs' effect, the solenoidal basis functions for the velocity field are matched to the interface. Namely, the stream function is approximated by the second-order  $B$ -splines [21] on a rectangular mesh in  $(x, z)$  space, where  $z=y-f(t, x)$ . Therefore, the velocity component tangential to the interface can have a discontinuous normal derivative at  $y=f(t, x)$  in accordance with the stress continuity condition. The resulting velocity field decomposition has the following form:

$$\mathbf{u}(t, x, y) = \text{rot}(0, 0, \Psi(y) + \Phi(y) \sum \lambda_{ij}(t) L_i(x) L_j(z)), \quad (4)$$

where  $\Phi(y) = \sin^2(\pi y/H)$  is a "shape function" [21] providing the no-slip condition at the walls. The functions  $L_k$  are one-dimensional second-order  $B$ -splines. As far as the second item on the right-hand side of Eq. (4) provides only a null total flow rate through the channel, the first item  $\Psi(y) = Q[3(y/H)^2 - 2(y/H)^3]$  specifies the constant dimensionless volumetric flow rate  $Q$  for the whole two-phase flow. In general, there is some freedom in choosing the functions  $\Phi$  and  $\Psi$ , because the sum over  $B$ -splines will anyway provide an approximation of a given solenoidal velocity field, having total flow rate  $Q$  and vanishing at the wall. It is recommended, however, to choose  $\Phi$  and  $\Psi$  being smooth and having as small gradients as possible. The ones, chosen above, are among the simplest appropriate representatives.

The code has been validated in the problem of a flat liquid film driven by gas flow, which has an exact solution with piecewise parabolic profile. The common procedure of mesh refinement has also been used throughout the calculations. The parameters of the numerical scheme are chosen to provide a difference of about 1% when both the space and time resolutions are doubled.

We only consider here the case of a thin film in a large channel, so we assign  $H=10h$  in all calculations (Fig. 1). We also fix the ratios  $\rho_2/\rho_1=10^{-3}$  and  $\nu_2/\nu_1=10$  and the Weber number  $We=10^4$ , which approximately corresponds to the air/water system with about a 130- $\mu\text{m}$ -thick film. One of the main goals of this paper is to compare shear driven waves with gravity (or any other body force) driven waves. In order to have a pure case of a single external force, we neglect gravity in the calculations for shear driven waves in the present research. In practice, this situation may arise either

for very thin films over a vertical wall, when the Galileo number  $G$  is small as compared to the shear stress, or for film flows in microgravity, where the shear is an attractive alternative as a driving force. Thus, there remain just two dimensionless parameters of the problem: a volumetric flow rate  $Q$ , which accounts for the shear stress, and the dimensionless length of the domain,  $L$ , which is actually the wavelength. It should be noted that liquid film flow is much thinner and much slower than gas flow; therefore, its volumetric flow rate is of the order of  $10^{-3}$  of that for gas. Therefore,  $Q$  is practically equal to the gas flow rate and the Reynolds number for the gas flow is  $Re_g = Q\nu_1/\nu_2$ .

The results on the gravity driven waves, presented below for the sake of comparison, are obtained for the film falling down a vertical wall—i.e., for the vector  $\mathbf{e}_g$  directed along the bottom—without ambient gas and at the same fixed  $We=10^4$ . Thus, there are also just two parameters: Galileo number  $G$ , which accounts for the driving force, and the wavelength  $L$ .

All calculations are started from the film being at rest. Its thickness at  $t=0$  is slightly disturbed according to  $f(0, x) = 1 + 0.05 \cos(2\pi x/L)$ . The gas Reynolds number for the discussed below results on stationary waves is within the range of  $Re_g=600-1700$ . When  $Re_g$  is low, the disturbances may decay or they may lead to wave motion, but the latter remains nonstationary. A detailed study of long-wave instability can be found elsewhere [8,9], and it is beyond the scope of this paper. We give here just two examples for illustration. For  $L=100$  the initial disturbances decay at  $Re_g=330$  but they grow at  $Re_g=500$ , which is in agreement with experimental stability diagram [15] for the air/water system in a thin channel with close aspect ratio  $H/h$ . For  $L=400$  the wave motion is nonstationary at  $Re_g=580$ , but at  $Re_g=650$  stationary solitary waves appear. It is worth mentioning also that a linear analysis (Ref. [9], Fig. 8) predicts the wavelength of the preferred mode to be about  $L=90$  for a water film of thickness 200  $\mu\text{m}$  at  $Re_f=7$ , which is close to the wavelengths and film Reynolds numbers considered in the present research.

While increasing  $Re_g$ , the stationary waves evolve from almost sinusoidal waves to nonsymmetric ones and then to the solitary waves [Fig. 2(a)]. The latter have shape and phase speed practically independent of the length  $L$  of computational domain for  $L \geq 200$ . The Reynolds number of the film flow,  $Re_f$ , is calculated directly as the dimensionless volumetric flow rate averaged over the wave period. Figure 2(b) shows a comparison between profiles of the gravity-

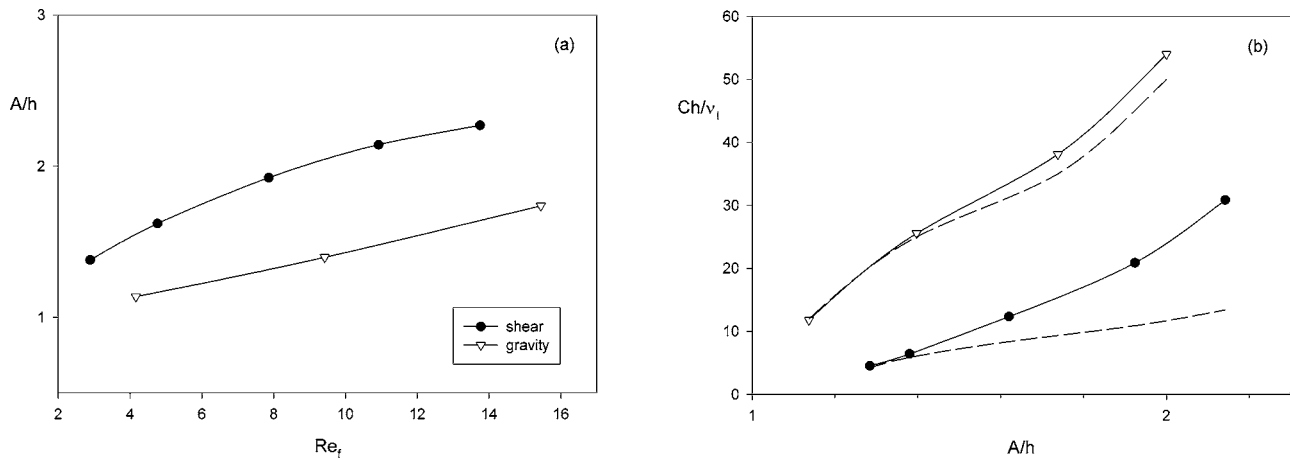


FIG. 3. Comparison between characteristics of shear driven and gravity waves for  $L=100$ : (a) amplitude  $A/h=\max f(t,x)$  versus film Reynolds number  $Re_f$  and (b) phase speed  $C$  versus amplitude. Dashed lines indicate the phase speed of the linear kinematic waves.

capillary solitary wave and the shear driven one of equal amplitude (earlier [20], the shape of calculated gravity-capillary solitary wave was shown to be in excellent agreement with Kapitza and Kapitza's experiment [1]). One can see that waves of different origins are generally similar. Still, the shear driven wave has a steeper backward slope, more mildly sloping front, and quite a different precursor capillary wave train.

A much greater difference can be observed as the amplitude and wave speed are concerned. Figure 3(a) shows that at equal values of  $Re_f$ , the shear driven waves are much higher. On the other hand, they are much slower as compared to the gravity waves of the same amplitude [Fig. 3(b)]. Comparison between the waves for  $L=200$  leads to a qualitatively similar result. Dashed lines show the phase speed for the linear kinematic waves—that is,  $C_0 h / v_1 = G$  for the gravity waves [2] and  $C_0 h / v_1 \approx 6Q\mu \frac{Hh^2(H+h)}{(H-h)^4} \approx \frac{H+h}{H-h} u_{int}$  for the gas driven waves when  $\mu = \rho_2 v_2 / \rho_1 v_1 \ll 1$ , where  $u_{int}$  is the dimensionless velocity at the interface. The latter expression follows from the mass conservation equation  $f_t + q_x = 0$ , where the dimensionless liquid flow rate  $q$  can be found from an exact solution of the flat film flow driven by gas. It reads  $q \approx Q\mu \frac{3Hh^2+h^3}{(H-h)^3}$  for  $\mu = \rho_2 v_2 / \rho_1 v_1 \ll 1$ . The plot in Fig. 3(b) may give a misleading impression that the phase speed of linear kinematic waves depends on  $A$ . The point is that there is a one-to-one correspondence between the amplitude  $A$  of stationary waves and driving force (shear stress or body force). And  $C_0$  is the speed of kinematic waves that would appear if this force were applied to the flat film. One can see that nonlinear waves inherit the distinction between phase speeds of linear kinematic waves for shear driven and gravity flows.

It should be noted that all observed shear driven waves, as well as gravity waves, are supercritical; i.e., their phase velocity is greater than phase velocity of linear kinematic waves [Fig. 3(b)]. For weakly nonlinear waves this difference is small but it grows significantly with increasing amplitude. We did not observe “slow” shear driven waves, which were reported in Refs. [12,18]. Our results for nonlinear waves qualitatively agree with the results of linear stability analysis [9], where all the unstable long waves are super-

critical. The wave speed of the largest long waves measured in Ref. [14] was also always 2–3 times larger than the velocity at the interface, the latter being equal to the phase speed of linear kinematic waves for  $H \gg h$ .

It should be noted that the numerical experiment described above is different from laboratory experiments [1–3] on the investigation of stationary gravity waves. The latter deal with “spatial” evolution of forced waves on a film falling down an inclined or vertical substrate. Here we simulate this flow considering “temporal” evolution of waves in a periodical domain. A similar approach for gravitational waves was earlier used in Refs. [5,6,20]. The main difference is that in numerical calculations the mean film thickness is preserved, while the mean flow rate (averaged over the wave period) is variable until the stationary waves saturate. The situation in laboratory experiments is the opposite. Keeping this in mind, one can compare calculated results with those obtained in experiments. It was shown (Ref. [2], Fig. 8.18)

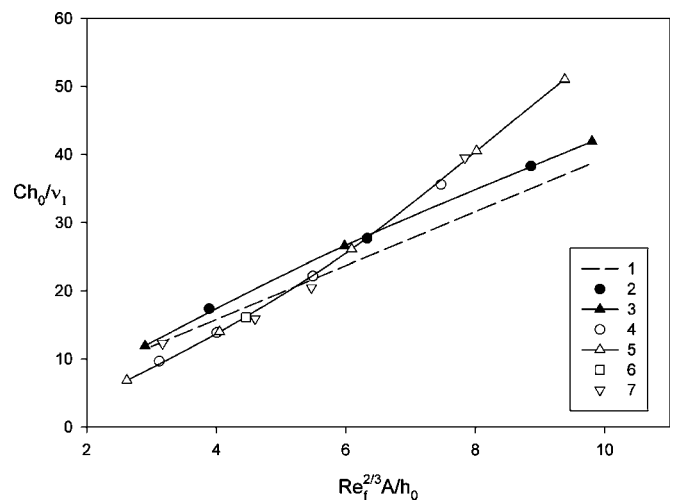


FIG. 4. Universal dependence of the phase speed on the properly scaled amplitude (see text and previous figure for the notations) (1) best fit to the experiment on gravity waves ([2], Fig. 8.18). Calculations of gravity waves: (2)  $L=200$  and (3)  $L=100$ . Calculations of shear driven waves: (4)  $L=200$ , (5)  $L=100$ , (6)  $L=400$ , and (7)  $L=50$ .

that proper scaling gives a universal linear dependence of the phase speed on the wave amplitude for gravitational waves on a vertical film, regardless of their wavelength. This dependence is plotted in Fig. 4 as a dashed line. Our calculations for gravity driven waves give close results. The discrepancy is within the limits of previously reported [5,6,20] difference between experiments and calculations. Here  $h_0$  is the thickness of flat Nusselt flow that has the same flow rate (Reynolds number) as stationary wave flow—i.e., the thickness that an initial part of film flow would have in an experiment. For the shear driven waves  $h_0$  is also the thickness of flat film flow driven by gas with the same  $Re_f$  as the corresponding stationary wave flow. The main result in Fig. 4 is that the phase velocity of such waves also exhibits a universal dependence, with the only exception being the shortest

waves ( $L=50$ ) of small amplitude. And this dependence is quite different from that for gravity waves.

In summary, we have numerically investigated nonlinear stationary traveling waves on a thin liquid film driven by gas flow. It has been shown that there exist solitary shear driven waves. They have slightly different shape and much smaller phase speed as compared to gravity-capillary waves of the same amplitude. They also have much greater amplitude at the same magnitude of film Reynolds number. All the obtained shear driven waves are supercritical. We have not observed “slow” waves reported in Refs. [12,18]. The universal dependence of the phase speed on the wave amplitude (both specially scaled) is revealed.

This work was supported by a grant of the Siberian Division of RAS, interdisciplinary project No. 111.

- 
- [1] P. L. Kapitza and S. P. Kapitza, *Zh. Eksp. Teor. Fiz.* **19**, 105 (1949).
- [2] S. V. Alekseenko, V. A. Nakoryakov, and B. G. Pokusaev, *Wave Flow of Liquid Films* (Begell House, New York, 2001).
- [3] J. Liu and J. P. Gollub, *Phys. Fluids* **6**, 1702 (1994).
- [4] M. Vlachogiannis and V. Bontozoglou, *J. Fluid Mech.* **435**, 191 (2001).
- [5] T. R. Salamon, R. C. Armstrong, and R. A. Brown, *Phys. Fluids* **6**, 2202 (1994).
- [6] B. Ramaswamy, S. Chippada, and S. W. Joo, *J. Fluid Mech.* **325**, 163 (1996).
- [7] N. A. Malamataris, M. Vlachogiannis, and V. Bontozoglou, *Phys. Fluids* **14**, 1082 (2002).
- [8] B. S. Tilley, S. H. Davis, and S. G. Bankoff, *J. Fluid Mech.* **277**, 55 (1994).
- [9] R. Miesen and B. J. Boersma, *J. Fluid Mech.* **301**, 175 (1995).
- [10] T. M. Segin, B. S. Tilley, and L. Kondic, *J. Fluid Mech.* **532**, 217 (2005).
- [11] L. S. Cohen and T. J. Hanratty, *AIChE J.* **11**, 138 (1965).
- [12] A. D. D. Craik, *J. Fluid Mech.* **26**, 369 (1966).
- [13] L. A. Jurman and M. J. McCready, *Phys. Fluids A* **1**, 522 (1989).
- [14] C. A. Peng, L. A. Jurman, and M. J. McCready, *Int. J. Multiphase Flow* **17**, 767 (1991).
- [15] O. A. Kabov, Yu. V. Lyulin, I. V. Marchuk, and D. V. Zaitsev, *Int. J. Heat Fluid Flow* (to be published).
- [16] C. Kouris and J. Tsamopoulos, *Phys. Fluids* **14**, 1011 (2002).
- [17] J. Zhang, M. J. Miksis, S. G. Bankoff, and G. Tryggvason, *Phys. Fluids* **14**, 1877 (2002).
- [18] E. A. Demekhin, *Fluid Dyn.* **16**, 188 (1981).
- [19] A. M. Frank, *Discrete Models of Incompressible Fluid* (Fizmatlit, Moscow, 2001) (in Russian).
- [20] A. M. Frank, *Eur. J. Mech. B/Fluids* **22**, 445 (2003).
- [21] A. M. Frank, in *Notes on Numerical Fluid Mechanics and Multidisciplinary Design* (Springer, Berlin, 2005), Vol. 88, pp. 189–204.